

The Effect of a Partially Wetting Second Phase on Conduction

D.P. Birnie, III

The conduction behavior in a realistic three-dimensional two-phase microstructure is examined. Specifically, the case of a nonconducting, partially wetting second phase is examined. An electrical circuit analogue is used to quantitatively measure the effect. The dihedral angle that the second phase makes at grain boundaries is found to significantly influence the conductivity. As the second phase penetrates deeper into the grain boundary region, the conduction pathways are restricted to a greater degree. This is important for microstructures that result from a variety of standard processing techniques that involve the presence of liquid phases during heat treatment.

Keywords:
thermal conduction, electrical conduction, dihedral angle, composite/microstructure, grain boundaries, processing, sintering, sintering microstructure

1. Introduction

INTIMATELY mixed two-phase microstructures result from a number of different processing routes, notably liquid-phase sintering, glass ceramic fabrication, reactive sintering, etc. For many of these techniques, the final microstructure consists of one primary phase with a second phase holding the matrix grains together. Usually, the matrix phase is the constituent of interest, and the second phase is present only to facilitate processing. This second phase is often detrimental to the intended thermal or electrical conduction application.

The present analysis is performed for the case in which the secondary phase has a small dihedral angle and is significantly less conductive than the matrix phase; this is typical of most liquid-phase sintered microstructures.[1,2] The results apply to systems such as thermal conduction in sintered aluminum nitride substrates[3] and electrical conduction in sintered thick-film resistors.[4]

This article explores the effect of the shape of the secondary second phase on conduction behavior; the shape of this second phase is determined entirely by equilibrium capillary force balances established during high-temperature processing. The analysis applies generally to thermal conduction and to some specific cases of electrical conduction (as discussed later). The following section describes the basic features of equilibrium three-dimensional microstructure, as defined by the capillary force balances and the dihedral angle. Based on this description, a simple, reasonable representation of the three-dimensional microstructure is developed. The general behavior of conduction in this three-dimensional microstructure is then studied using an electrical circuit analogue. By varying the dihedral angle of the second phase constituent at grain boundaries, the effect of microstructure shape is determined. These effects are then cast into the form of linear mixing rules that are often used to represent the properties of composite materials; the effect of microstructure shape is found to have a significant effect on conduction through the composite material.

D.P. Birnie, III, Department of Materials Science and Engineering, University of Arizona, Tucson, Arizona

2. Background

The shape of second-phase particles in any equilibrium microstructure is governed by the force balance between different surface tensions acting at three-grain intersections. In particular, the arrangement of the grain boundary between two matrix grains is of interest (phase A) where it meets the second phase (B). This condition is illustrated in Fig. 1. The dihedral angle (θ_D) is the entire angle measured at the point of intersection of the grain boundary with the two interfaces. The angle is measured "inside" the second phase. The dihedral angle is determined by the grain boundary energy (γ_{AA}) and the interphase boundary energy (γ_{AB}):

$$\cos\left(\frac{\theta_D}{2}\right)=\frac{\gamma_{AA}}{2\gamma_{AB}} \quad [1]$$

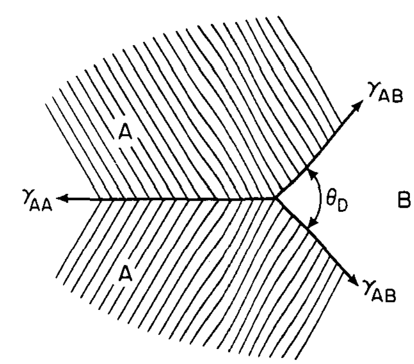

Fig. 1 Cross section of a three-grain junction between two grains of phase A and one grain of phase B. The dihedral angle is measured inside the second phase. It is determined by the two types of interface (A-A and A-B) that intersect at the junction and by their interfacial tensions (γ_{AA} and γ_{AB}).

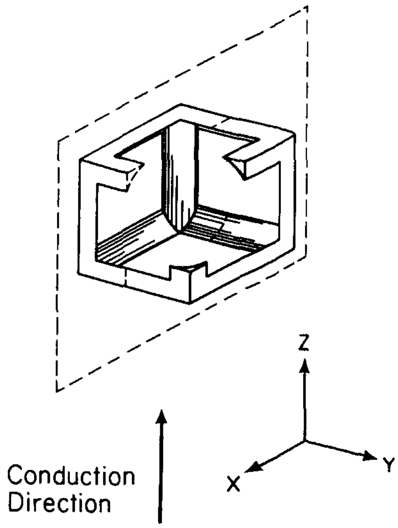

Fig. 2 Perspective cut of one grain in the simple cubic grain arrangement. The low dihedral angle interconnected second phase is shown.

When two phases are intimately mixed together, they form a microstructure that is determined only by the dihedral angle and by the volume fractions of each phase.[1,5-18] The grain size is important, but it only scales the size of the microstructure, not the shape. For a small dihedral angle, the second phase forms an interconnected microstructure; both the primary phase and the second phase are completely interconnected. At a large dihedral angle, the second phase exists as isolated pockets that are not interconnected.[5,17,18]

For the present analysis, only a very simple description of the grain packing is necessary. Shapes described in the following sections will arise from a simple cubic packing of grains, with the second phase distributed around the grain edges and corners and having an equilibrium dihedral angle with the grain boundary regions. Although the simple cubic packing geometry does not exactly model the true microstructure with random grain packing, it is somewhat better than fcc or bcc arrangements because the packing density in these other arrangements is higher than normally achieved for random grain [illegible]

[illegible] arrangement of grains, the second [illegible]

The π/2 limit applies because in this simple cubic packing four grains meet along each grain edge. In microstructures where the grain arrangement is more close packed, then only three grains will meet along grain edges. This will then define the cutoff limit at π/3 radians; this is more typical of real microstructures. Note that an interconnected microstructure will not occur for large dihedral angles. If a phase with a large dihedral angle initially existed along the grain edges, then it would be unstable to perturbations; it would decay into isolated pockets of second phase by Rayleigh fluctuations.[19,20]

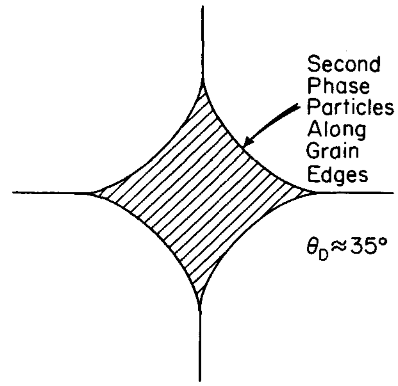

Fig. 3 Cross section of a four-grain junction in the simple cubic packing of grains. This star shape results whenever the dihedral angle is small.

A single cube of the low dihedral angle case is illustrated in Fig. 2. Shown is one matrix grain surrounded by the interconnected second phase along multigrain junctions. When the microstructure is interconnected (at a low dihedral angle), the cross section of the second phase along the grain edge will be a four-pointed star shape, as shown in Fig. 3. These shapes apply when the microstructure is kinetically able to reach equilibrium; this is applicable here because the second phase would have been liquid at high temperature. Other cases where fibrous phases are added for strengthening purposes will usually not be treated at high enough temperatures to reach capillary equilibrium.

If we consider the small dihedral angle case of this model grain network, then conduction along one of the cubic axes can be broken down into two components. The first component of conduction is through the second phase at grain edges that are parallel to the conduction direction. This amounts to one third of the total second phase that is present because grain edges point in all three directions. The second component of conduction is through the primary phase grains with their embedded second phases at the other (perpendicularly oriented) grain edges. These two conduction routes can be identified by examining Fig. 2. When considering conduction that is not parallel to one of the three axes, then it can be resolved into components [illegible] model and description used here will still apply.

The shape of the second phase will have no impact on conduction that is through second phases that are aligned with the conduction direction (one third of the second phase that is pre[illegible] conduction perpendicular to the remaining second phase material; the star-shaped cross section second phase protrudes much broader than a simple rod shape and might inhibit conduction more. This possibility is explored in detail using an electrical circuit analogue in the next section.

3. Experimental Procedure

Equilibrium microstructures have been analyzed above showing that, at low dihedral angle, some fraction of the con-

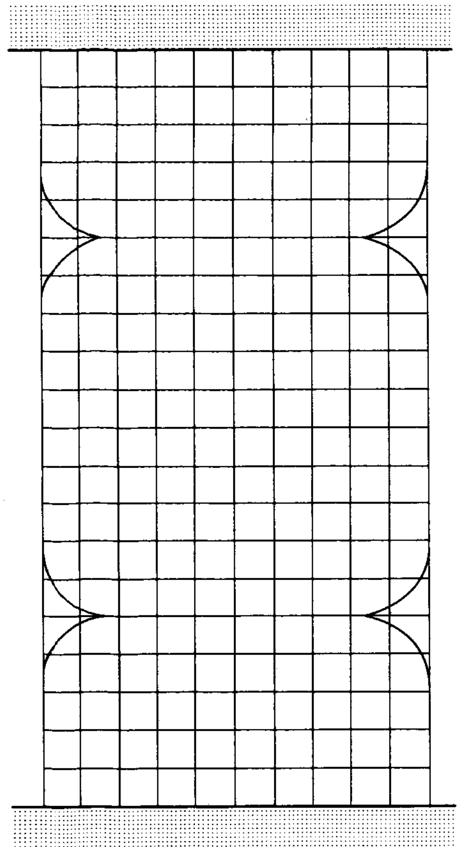

Fig. 4 Sample two-dimensional microstructure with 3% nonconductive second phase and a dihedral angle of π/6. The second phase penetrates between the adjacent grains significantly more than a circular second phase.

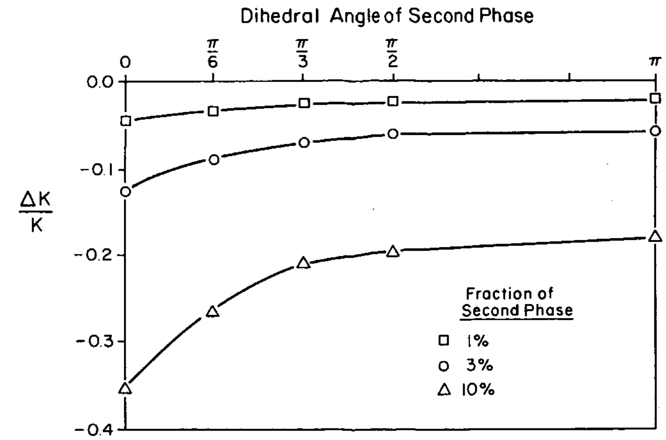

Fig. 5 Fractional change in conductance as a function of dihedral angle. Three values of the area fraction of second phase present are plotted as separate lines.

duction will occur in a mode that is perpendicular to fibrous second-phase particles (although fibers having star-shaped cross sections). The conduction in these microstructures is now measured using an electrical circuits analogue in two dimensions. Shapes are measured that correspond to the star-shaped continuous second phases that are found along multigrain junctions, as described above. Because the conduction pathway is around fibrous shapes, essentially in a single plane, then a two-dimensional analogue may be used with complete rigor.

A conductive polymeric film was used as a conductive two-dimensional medium. The film was polyethyleneterephthalate (PET) coated with a thin conductive coating (indium tin oxide, ITO). Rectangular pieces of this film were cut, and electrodes were attached to the two ends by clamping metal bars to the surface. This provided linear and parallel contacts to the material. This is identical to what would be found in a thick-film resistor geometry.[4,21] The conductance of the starting geometry was measured to eliminate any possible sample-to-sample variation in the conductance of the film. Then, segments of the film were removed with a razor blade to match a stencil representative of a given microstructure (defined by dihedral angle and area fraction). Stencils of different microstructures were generated on a plotter. The segments that were removed corresponded to the locations and shapes of the second-phase additions to the microstructure. Because only the remainder of the film provided a clear conduction path, this modeled the limiting case where the matrix was much more conductive than the second-phase addition. After these film sections were removed, the conductance was again measured. To ensure accurate results, the electrodes were not removed between measurements.

Stencils were designed to represent the conduction in series through two square grains; two grains were used in series to reduce any effect of electrode placement. This modeled a cross section through the simple cubic grain geometry described above. Because the grain boundary region is the typical location of the second-phase particles, the stencils were designed such that the electrical flow would start at the center of a grain, then pass through two grain boundary regions, and finally conduct to the center of a third grain. The conduction distance was then two grain diameters. This required the formation of stencils with a 2:1 aspect ratio. The second-phase additions were constrained to have a given dihedral angle and area fraction; they were placed at four-grain junctions, their preferred location. Due to the symmetry of the current flow, the particles were placed on the edges of the stencils; this also simplified the excision of that segment of film during the conductance measurement.

Figure 4 shows a sample film stencil for a microstructure with 3% second phase and a dihedral angle of π/6. For this small dihedral angle, the second phase penetrates significantly into the grain boundary region. This shape of second-phase particle extends much further than a particle of the same area that is circular. Therefore, the current will have to travel further around it; resistive second phases that penetrate deeply into the grain boundary are expected to be a greater impediment to conduction than localized phases.

Data were obtained for three values of area fraction and for several values of the dihedral angle. The dihedral angle ranged between 0 and π radians. These limits correspond to a completely wetting second phase (like that required for liquid-phase sintering)[1,2] and a completely nonwetting second phase (modeled here in two dimensions as the circular cross section of a fibrous second phase).

4. Results

The initial conductance values provide a measure of the sample-to-sample variation in the starting material. The sheet conductance was 0.0076 ± 0.0006 squares/Ohm, averaging all samples tested. The fractional change in the conductance gives a measure of how strongly the second phase affects the conductivity of the sample. The results are plotted in Fig. 5. It can be seen that the particles that had the smallest dihedral angle caused a significant decrease in the conductance of the film (about a factor of two times worse for the same area fraction of second phase). Three-dimensional conduction properties can be deduced from these results, as discussed further in the next section.

5. Discussion

Conduction through composite microstructures is often dealt with in one of two extremes: in the parallel limit or the series limit. The conductivity mixing rules for these two simple cases are

Parallel:

$$K_{mix} = x_A K_A + x_B K_B \qquad [2]$$

Series:

$$K_{mix} = \frac{K_A K_B}{x_A K_B + x_B K_A} \qquad [3]$$

where x_A is the volume fraction of the primary phase, and x_B is for the secondary phase. All volume must be accounted for, so $(x_A + x_B) = 1$ must be satisfied. In the parallel case, the conduction is dominated by the more conductive phase, whereas the series case is dominated by the less conductive material.

As presented in the background, real microstructures fall somewhere between these two extremes; some of the microstructure will be parallel to the conduction direction and some will be in series. The above two equations will be limiting cases that bound the thermal conductivity of a mixture of two phases.[22,23]

Table 1 Conductance changes for two-dimensional films with circular, nonconducting second phases of varying volume fraction

Area fraction	Conductance ratio measured	Conductance ratio Predicted from Eq 5
0.10	–0.182	–0.182
0.03	–0.060	–0.058
0.01	–0.022	–0.020

Note: Measured and theoretical values are compared.

Two other useful solutions are for spherical second-phase particles and for conduction perpendicular to rod-shaped particles. The spherical second phase case would apply when the dihedral angle is very large, causing the second-phase particles to be in isolated pockets with nearly spherical shape, whereas the solution for conduction around rod-shaped particles would apply for a fiber-reinforced composite. The mixing rules for these shapes are

Around spheres:

$$K_{mix} = K_A \frac{2(1 - x_B) K_A + (1 + 2x_B) K_B}{(2 + x_B) K_A + (1 - x_B) K_B} \qquad [4]$$

Perpendicular to fibers:

$$K_{mix} = K_A \frac{(1 - x_B) K_A + (1 + x_B) K_B}{(1 + x_B) K_A + (1 - x_B) K_B} \qquad [5]$$

For geometries that are intermediate between spheres and rods, ellipsoidal shapes have been used. These approximations yield solutions that are intermediate between these cases.[24-33] However, in none of these cases is dihedral angle of the second phase used in solving the conduction equations; this solution would be difficult due to the sharp corners where the second phase penetrates between grains. This made the above electrical circuit analogue an attractive way to determine the importance of grain shape on conductivity.

The second phases that are oriented perpendicularly to the conduction direction will affect the primary phase conductivity in approximately the manner of the fibrous second-phase additions described in Eq 5. However, in this microstructure, the cross section of the second phase will not be circular. It will have the star shape shown in Fig. 3; it will offer a different level of impediment to conduction than a simple circular cross section fiber. Therefore, the composite microstructure will have a conductivity that is determined by parallel conduction through the fraction of phase B (one third of x_B), which is aligned along the direction of conduction (having conductivity K_B), and the remainder of the material (having conductivity K_{mix}). Using Eq 1 for parallel conduction, the total conductivity of the composite microstructure will be

$$K_{total} = \left(1 - \frac{x_B}{3}\right) K_{mix} + \frac{x_B}{3} K_B \qquad [6]$$

Table 2 Shape enhancement factor as a function of dihedral angle

Dihedral angle	Shape enhancement factor
0	2.10
π/6	1.52
π/3	1.20
π/2	1.03
π	1.00

Note: Data are experimental data taken with 3% nonconductive second phase.

where K_{mix} will depend on K_A, K_B, and the dihedral angle. The component of flow through phase B in this equation does not depend on the dihedral angle because this flow is through this phase, not around it.

The conductivity for the remaining mixture was evaluated above (as a function of the dihedral angle) using the electrical circuit analogue. The data obtained in this experiment demonstrate the level of amplification of conduction interference by the penetrating second phases, in comparison with perfectly round fibers.

The experimentally determined conductivity changes can be validated by comparison with Eq 5. The data for the circular second phases in two dimensions ($\theta_D = \pi$) apply exactly to the case of conduction normal to rod-shaped fibers. Table 1 shows this comparison; the measured and calculated change in the conductance is very close. This confirms that the electrical circuit analogue is accurate at determining changes in conductivity.

Other second-phase shapes offer different levels of impediment to conduction. This is shown in Fig. 5; particles with dihedral angles equal to zero had about two times the effect on the conductance compared to the circular cross section second phases. Table 2 quantifies the 3% line from Fig. 5. The "shape enhancement factor" is the ratio of the conductance reduction at the given dihedral angle compared to that for $\theta_D = \pi$.

The change in conductance was very flat over a wide range of larger values of the dihedral angle. The data for larger dihedral angles ($\theta_D > \pi/4$) are all very similar to the data for the exactly circular ($\theta_D = \pi$) cross section second phase. From this, it can be inferred that isolated pockets of second phase will behave very similarly to spherical second-phase inclusions. Therefore, only the low dihedral angle microstructure case will be significantly impacted by differences in dihedral angle. However, these cases are of most interest to explain microstructures that develop at high temperatures.

This shows that wetting second phases will have a significant effect in reducing the macroscopic conductivity of aggregate samples. The effect will be significant, particularly in samples derived from a liquid-phase sintering route, where the dihedral angle must be zero.

Note that the present simulation is focused on materials where there is no specific conduction impediment at the grain boundary. This is certainly representative of thermal conduction; the mean free path for phonons is typically much smaller than the grain size. However, some caution may be required when using this geometry for electrical applications,[34,35] particularly in semiconducting materials that may have space charge layers at grain boundaries.[36]

It is anticipated that many different systems and properties can be influenced by the microstructure (and specifically the dihedral angle of the second phase). The present derivation and measurement of the small dihedral angle case can be applied to many microstructures that might arise from liquid-phase sintering or other processing routes. One example is thermal conduction in aluminum nitride; the matrix is much more conductive than the second-phase sintering additives. These additives wet the grain boundaries ($\theta_D = 0$) so that the shape enhancement effects must be considered.

6. Conclusions

Different simple mixing rules for properties of two-phase composites have been examined. These mixing rules have been extrapolated to a realistic three-dimensional microstructure; second-phase shapes in this microstructure are controlled by the dihedral angle that this phase makes at the grain boundaries of the matrix phase. The effect of second-phase shape in this microstructure has been tested using an electrical circuit analogue applicable to the case where the matrix is much more conductive than the second-phase additive. For dihedral angles near zero (typical of liquid-phase sintered microstructures), the second-phase particles are approximately two times as effective at reducing the conduction than the same volume fraction of particles that have a large dihedral angle. However, only the low dihedral angle case will be impacted to any measureable degree.

References

1. R. Raj, Morphology and Stability of the Glass Phase in Glass-Ceramic Systems, *J. Am. Ceram. Soc.*, Vol 64, 1981, p 245-248
2. W.D. Kingery, Densification During Sintering in the Presence of A Liquid Phase. I. Theory, *J. Appl. Phys.*, Vol 30, 1959, p 301-306
3. K. Komeya and H. Inoue, Sintering of Aluminum Nitride: Particle Size Dependence of Sintering Kinetics, *J. Mater. Sci.*, Vol 12, 1969, p 1045
4. M. Oakes, An Introduction to Thick Film Resistor Trimming by Laser, *Opt. Eng.*, Vol 17, 1978, p 217-224
5. C.S. Smith, Grains, Phases, and Interfaces: An Interpretation of Microstructure, *Trans. AIME*, Vol 175, 1948, p 15-51
6. W.D. Kingery, H.K. Bowen, and D.R. Uhlmann, *Introduction to Ceramics*, 2nd ed., Wiley, 1976, p 214
7. W. Beere, A Unifying Theory of the Stability of Penetrating Liquid Phases and Sintering Pores, *Acta Metall.*, Vol 23, 1975, p 131-138
8. W. Beere, The Intermediate Stage of Sintering, in *Vacancies '76*, R.E. Smallman and J.E. Harris, Ed., The Metals Society, 1976, p 149-155
9. J.R. Bulau and H.S. Waff, Mechanical and Thermodynamic Constraints on Fluid Distribution in Partial Melts, Vol 84, 1979, p 6102-6108
10. A. Toramaru and N. Fujii, Connectivity of Melt Phase in a Partially Molten Peridotite, *J. Geophys. Res.*, Vol 91, 1986, p 9239-9252
11. N. von Bargen and H.S. Waff, Permeabilities, Interfacial Areas and Curvatures of Partially Molten Systems: Results of Numerical Computations of Equilibrium Microstructures, *J. Geophys. Res.*, Vol 91, 1986, p 9261-9276
12. G.W. Greenwood, Some Geometrical Aspects of Microstructural Stability, *J. Mater. Sci.*, Vol 17, 1982, p 2127-2132
13. M.O. Tucker, A Simple Description of Interconnected Grain Edge Porosity, *J. Nucl. Mater.*, Vol 79, 1979, p 199-205
14. P.J. Rinous, M.O. Tucker, and A.G. Crocker, The Stability of Interconnected Pores in Materials of Non-uniform Grain Size, *Proc. Roy. Soc. London A*, Vol 382, 1982, p 201-220
15. I.V. Nicolaescu and F. Glodeanu, Pore Geometry and Interfacial Energy, *J. Nucl. Mater.*, Vol 113, 1983, p 253-255

16. D.P. Birnie, III and W.D. Kingery, The Influence of Partially Wetting Liquid Additions on Creep, *Ceram. Trans.*, Vol 7, 1990, p 477-491
17. P.J. Clemm and J.C. Fisher, The Influence of Grain Boundaries on the Nucleation of Secondary Phases, *Acta Metall.*, Vol 3, 1955, p 70-73
18. P.J. Wray, The Geometry of Two-Phase Aggregates in Which the Shape of the Second Phase is Determined by its Dihedral Angle, *Acta Metall.*, Vol 24, 1976, p 125-135
19. W.C. Carter and A.M. Glaeser, Dihedral Angle Effects on the Stability of Pore Channels, *J. Am. Ceram. Soc.*, Vol 67, 1984, p C124-C127
20. M.D. Drory and A.M. Glaeser, The Stability of Pore Channels: Experimental Observations, *J. Am. Ceram. Soc.*, Vol 68, 1985, p C14-C15
21. R.D. Jones, *Hybrid Circuit Design and Manufacture*, Marcel Dekker, 1982
22. S.R. Coriell and J.L. Jackson, Bounds on Transport Coefficients of Two-Phase Materials, *J. Appl. Phys.*, Vol 39, 1968, p 4733-4736
23. R.H.T. Yeh, Variational Bounds of Transport Properties of Composite Materials, *J. Appl. Phys.*, Vol 41, 1970, p 224-226
24. R.W. Cohen, G.D. Cody, M.D. Coutts, and B. Abeles, Optical Properties of Granular Silver and Gold Films, *Phys. Rev. B*, Vol 8, 1973, p 3689-3701
25. W.R. Tinga, W.A.G. Voss, and D.F. Blossey, Generalized Approach to Multiphase Dielectric Mixture Theory, *J. Appl. Phys.*, Vol 44, 1973, p 3897-3902
26. W.Y. Hsu and T. Berzins, Percolation and Effective-Medium Theories for Perfluorinated Ionomers and Polymer Composites, *J. Poly. Sci.*, Vol 23, 1985, p 933-953
27. D. Stroud, Generalized Effective-Medium Approach to the Conductivity of an Inhomogeneous Material, *Phys. Rev. B*, Vol 12, 1975, p 3368-3373
28. D. Stroud and F.P. Pan, Self-Consistent Approach to Electromagnetic Wave Propagation in Composite Media: Application to Model Granular Metals, *Phys. Rev. B*, Vol 17, 1978, p 1602-1610
29. M.H. Cohen, J. Jortner, and I. Webman, Percolation Conductivity in Granular Metal Films, *Phys. Rev. B*, Vol 17, 1978, p 4555-4557
30. H. Seki, Effective Medium Analysis of TeO_x Optical Storage Layers, *Appl. Phys. Lett.*, Vol 43, 1983, p 1000-1002
31. Z. Hashin and S. Shtrikman, A Variational Approach to the Theory of the Effective Magnetic Permeability of Multiphase Materials, *J. Appl. Phys.*, Vol 33, 1962, p 3125-3131
32. H. Fricke, The Maxwell-Wagner Dispersion in a Suspension of Ellipsoids, *J. Phys. Chem.*, Vol 57, 1953, p 934-937
33. R.E. Meredith and C.W. Tobias, Conduction in Heterogeneous Systems, in *Advances in Electrochemistry and Electrochemical Engineering*, Vol 2, C.W Tobias, Ed., Interscience, 1962, p 15-48
34. R.J. Macdonald, *Impedance Spectroscopy, Emphasizing Solid Materials and Systems*, John Wiley & Sons, 1987
35. P.G. Bruce and A.R. West, The A-C Conductivity of Polycrystalline LISICON $Li_{(2+2x)}Zn_{(1-x)}GeO_4$, and a Model for Intergranular Constriction Resistance, *J. Electrochem. Soc. Solid-State Sci. Tech.*, Vol 130, 1983, p 662-669
36. T. Takemura, M. Kobayashi, Y. Takada, and K. Sato, Effects of Bismuth Sesquioxide on the Characteristics of ZnO Varistors, *J. Am. Ceram. Soc.*, Vol 69, 1986, p 430-436